



Missouri University of Science and Technology
Scholars' Mine

International Specialty Conference on Cold-Formed Steel Structures

(1994) - 12th International Specialty Conference on Cold-Formed Steel Structures

Oct 18th, 12:00 AM

Design of a Purlin System

C. Jiang

D. St. Quinton

Follow this and additional works at: <https://scholarsmine.mst.edu/isccss>

 Part of the [Structural Engineering Commons](#)

Recommended Citation

Jiang, C. and St. Quinton, D., "Design of a Purlin System" (1994). *International Specialty Conference on Cold-Formed Steel Structures*. 4.

<https://scholarsmine.mst.edu/isccss/12iccfss/12iccfss-session8/4>

This Article - Conference proceedings is brought to you for free and open access by Scholars' Mine. It has been accepted for inclusion in International Specialty Conference on Cold-Formed Steel Structures by an authorized administrator of Scholars' Mine. This work is protected by U. S. Copyright Law. Unauthorized use including reproduction for redistribution requires the permission of the copyright holder. For more information, please contact scholarsmine@mst.edu.

Design of a Purlin System

J M Davies¹, C Jiang¹ and D St Quinton²

Introduction

This paper is concerned with the design of cold-formed steel structural members which span between the frames of a building and carry cladding which is usually either single- or double-skin profiled metal sheeting or a sandwich panel. The cladding is fixed to these purlins or sheeting rails at regular intervals and the performance in service, and therefore the design, is strongly influenced by interaction with the sheeting. The connection between the purlins and the supporting structure also has a significant influence on performance so that, historically, the emphasis has tended to be on empirical methods of design rather than detailed calculations of the structural behaviour.

In a previous paper[1], the first author described the design of a purlin system, known as Multibeam Mark 2, based on a cold-formed steel Sigma profile. The alternative approaches to design were reviewed and a semi-empirical design procedure was described which resulted in safe but competitive load-span tables. This paper describes the design of Multibeam Mark 3. This involves a further evolution of the cross-section together with further improvement of the design procedure. The tendency is to continue to move away from reliance on testing and towards an approach which is much more orientated towards design by calculation, a trend which is becoming increasingly necessary in view of the proliferation of different cladding types, all offering different degrees of restraint to the purlin. It is shown that, in the present state-of-the-art, a design procedure based entirely on calculation, while taking into account such practical factors as restraint from alternative cladding systems and distortion and partial plasticity at internal supports, is now feasible. However, as the profession may not yet be ready for such a radical approach, the design procedure used for Multibeam Mark 3 is backed up by a comprehensive test programme.

Evolution of purlin cross-sections

In the UK, a small number of manufacturers dominate the market and there are only a small number of cold-formed purlin sections to be considered. There are two basic shapes, the Zed and the Channel and these have evolved as shown in Fig.1.

The principal axis of a Zed purlin is typically inclined at about 17° to the web and, unless the load is applied in the direction of the principal axis, a Zed purlin is subject to bi-axial bending. With a typical roof slope of about 6°, there is an appreciable angle between the line of action of the load (vertical for snow, normal to the roof for wind) and the principal axis so that a significant bi-axial bending effect tends to occur. In practice, the cladding acts as a relatively rigid diaphragm and absorbs the minor axis bending tendency in the form of an in-plane load. This in-plane load can be quite large and must be adequately resisted or

¹ Telford Research Institute, University of Salford, Salford M5 4WT, UK.

² Ward Building Systems, Sherburn, N. Yorkshire YO17 8PQ, UK.

else the purlins will roll over at quite low levels of applied load. The 'Zeta' purlin is designed to avoid the major disadvantage of the simple Zed by bringing the inclination of the principal axis much closer to the roof slope. A typical Zeta section has its principal axis inclined at about 7° to a line drawn normal to the flanges so that, in many roofs, the principal axis is near vertical. It follows that this section is much less prone to twisting at the erection stage and would also be expected to show improved performance when interacting with the cladding in its working configuration.

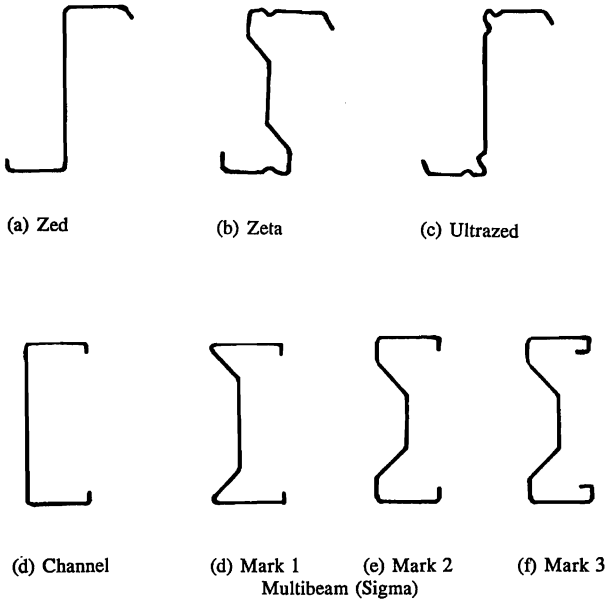


Fig.1 Evolution of cold-formed purlin sections

The many bends in the Zeta and Ultrazed sections have the advantage that they make the sections very resistant to local buckling. Despite their complexity, these sections maintain the inherent capacity of the Zed section to nest and overlap.

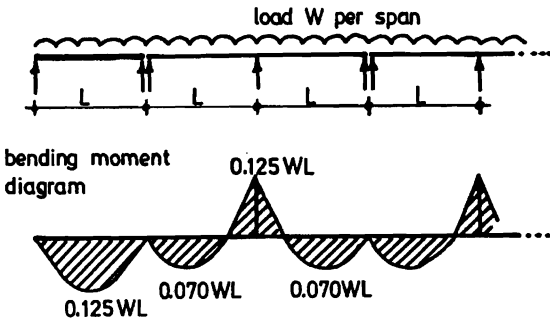
The Multibeam is a long-standing improvement of the simple lipped channel. The main disadvantage of conventional channel profiles is that the shear centre lies outside the section so that load applied through the flange resolves itself into a load through the shear centre together with an applied torsion. Cold-formed channel sections therefore exhibit a pronounced tendency to twist. The Multibeam section avoids this by folding the web to bring the shear centre into the section. The additional web bends also serve to stabilise the section against local buckling of the web.

Multibeam has now passed through the three stages of evolution shown in Fig. 1. Mark 3, which is the subject of this paper, has improved section properties for a given weight per unit length, largely as a consequence of the double lip.

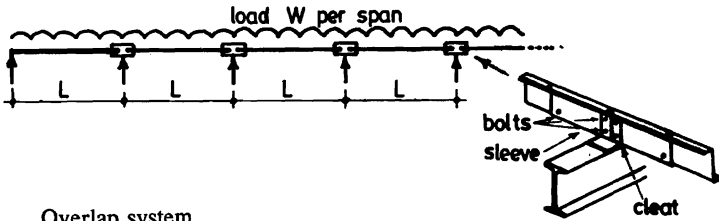
Purlin Systems

Purlin and side rails usually form long runs of members over a number of equally spaced supports. Practical considerations rule out attempts to obtain full continuity of bending action so that proprietary purlin design tends to appeal to partial continuity. The major possibilities are summarised in Fig.2 and, in each case, it will be observed that the end span requires separate consideration. It is evident that with a double span system, when a structure has an odd number of bays, there must be a single span case at one end of each line of purlins. When the number of bays is even, it is important to realise that it is still necessary to stagger the joints as shown in Fig. 3 in order to equalise the loads on the frames. If this is not done, alternate frames will be much more heavily loaded as a consequence of the internal support reactions being significantly greater ($1.25 WL$) than two end reactions ($0.75 WL$).

1. Simple system



2. Sleeve system



3. Overlap system

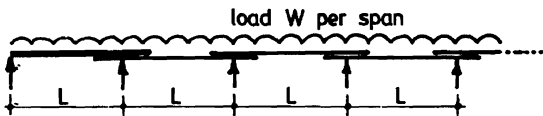


Fig.2 Purlin systems

The main characteristics of the alternative systems may be summarised as follows:

- (1) Simple system. This is based on the use of two-span lengths of purlin, except for the special case of the end bays. The intention is to economise on fabrication while being prepared to use slightly heavier sections than with some of the alternative systems which achieve a higher degree of continuity. The simple system is particularly appropriate for shorter spans.

The design of a simple two-span system is dominated by the large bending moment at the central support. However, when a two-span arrangement is subject to test, it is clear that there is a considerable capacity for redistribution of bending moment so that an elastic analysis is quite inappropriate as a basis for two-span purlin design. Indeed, some of the more compact cold-formed purlin sections with well-designed cleats at the internal supports are capable of carrying loads approaching close to those predicted by plastic theory. It follows that economical purlin design necessitates consideration of partial plasticity at the internal supports and this has traditionally involved testing. The safe load tables provided by the manufacturers of the more successful purlin systems have all been derived from the results of extensive test programmes.

- (2) Single span sleeve system. This system uses a short extra length of stiffening in order to achieve a degree of continuity at each internal support. With Zed sections, the sleeve can take the form of an offcut of the basic purlin. With the sigma section, a purpose made sleeve is required. In each case, the basic cleat arrangement is essentially unchanged, the sleeve being an extra component introduced into the typical connection at a cost of a short extra length of cold-formed member and two or more additional bolts.

Consideration of the shape of the bending moment diagram reveals that only partial continuity at the sleeve is required and indeed that too high a degree of continuity could be positively harmful. The essence of sleeve design is therefore to tune the strength and stiffness of the complete connection in order to obtain the most favourable bending moment diagram.

- (3) Overlap system. The overlap system takes advantage of the fact that, if a Zed profile is rolled with one flange slightly wider than the other, the inverted profile will fit tightly inside the original. Consequently, if alternate spans are inverted, the profile will readily overlap. This ability to overlap can be facilitated by splaying one lip slightly although this must be done with caution as the strength of a Zed profile can be surprisingly sensitive to the angle of splay.

The essential characteristic of overlap systems is to match strength to bending moment in an arrangement that achieves virtually full continuity. In the internal spans of a continuous beam, the support bending moment is precisely twice the mid-span moment and this in turn is precisely matched by the moment of resistance in a full strength overlap. The cut-off points are determined by the shape of the bending moment diagram and, obviously, the end span is in a heavier section in order to match the increased bending moment there.

Overlap systems can be designed largely without testing as there is no appeal to inelastic connection behaviour or redistribution of bending moment. It is, however,

necessary to establish that the overlap is fully effective and, as this involves a degree of mechanical interlocking, limited testing can be advantageous. Furthermore, as with all of these systems, it is necessary to consider the stability of the section under wind uplift when the unstabilised lower flange is in compression.

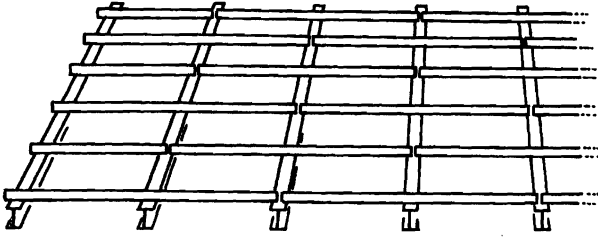


Fig.3 Staggered joints in a two-span purlin system

Design procedure used for Multibeam Mark 2

Multibeam Mark 2 had simple and sleeved variants both of which were designed on the basis of the collapse mechanism shown in Fig.4. The behaviour at the internal support is crucial and this was investigated using the simulated central support test defined in Fig. 5. The apparatus that was used was described in the earlier paper[1]. In carrying out this test, it was important to be able to determine the load-deflection relationship well into the drooping post-failure region and the test equipment was carefully designed to make this possible. The collapse load W_c of the two-span purlin was then predicted using the following equations:

$$W_c = \frac{2[M_2L + M_1(L - x)]}{x(L - x)} \quad (1)$$

$$\frac{x}{L} = \frac{(M_1 + M_2) - [(M_1 + M_2)^2 - M_1(M_1 + M_2)]^{\frac{1}{2}}}{M_1} \quad (2)$$

where the parameters in the equations are defined in Fig.4.

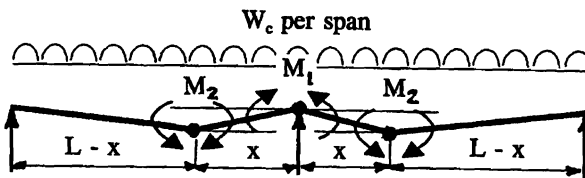


Fig.4 Collapse mechanism for two-span purlin

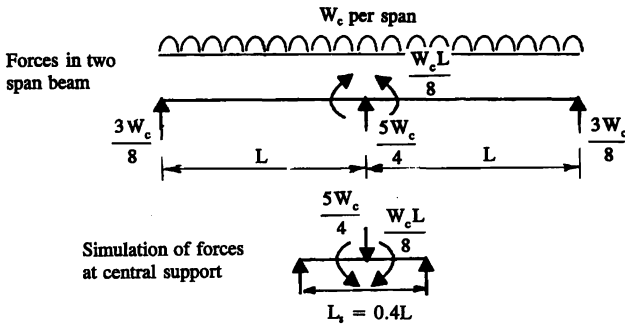


Fig.5 Simulated central support test

Having calculated the collapse load W_c , the plastic hinge rotation θ_p at the central support at collapse is given by

$$\theta_p = \frac{L}{1.5EI} \left[\frac{W_c L}{8} - M_1 \right] \quad (3)$$

where EI is the flexural rigidity of the purlin.

Investigation over a wide range of purlin sizes and spans showed that θ_p was generally in the range between 2° and 3° and that 3° represented a reasonable upper limit to the required rotation capacity. Accordingly, the design procedure for Multibeam Mark 2 was based on the above equations using the following steps:

- M_1 was determined experimentally using the simulated central support test defined in Fig.5. The required value was read off the drooping part of the load-deflection curve at a plastic hinge rotation of 3° .
- M_2 was determined experimentally on the basis of tests on simply-supported purlins clad with a representative steel sheeting profile using a vacuum test rig. Different values of M_2 were determined for downward and uplift loading.
- The ultimate load was determined using equations (1) and (2).
- The design procedure was confirmed by comparison with tests on two-span purlins under both downward and uplift load. The precision of the method was improved by an experimentally determined correction factor.

Improved design procedure for Multibeam Mark 3.

The above design procedure was evolved about eight years ago, and the passage of time had proved it to be extremely successful. A critical re-evaluation, however, suggested that in the light of subsequent developments some improvements could be made:

- As a result of improvements in techniques for the numerical analysis of cold-formed sections, the extensive demand for full-scale testing should be reduced.
- The evaluation of the support bending moment M_1 at collapse at a plastic hinge rotation of 3° was somewhat arbitrary and a more exact procedure should be used.
- Provision should be made for the design to cater for different cladding systems, particularly under wind uplift where the restraint from the cladding is crucial.

The following paragraphs show how these improvements were introduced.

Improved design equations

The load-deflection curves from the simulated central support tests were re-plotted in the form of central bending moment versus *plastic* rotation θ_p as shown in Fig.6. A conservative plastic moment-rotation line was then drawn on this graph in which M_1 is equal to the maximum bending moment M_{y1} at $\theta_p = 0$ and asymptotic to the drooping curve for higher values of θ_p . This line is given the equation

$$M_1 = M_{y1} - K \theta_p \quad (4)$$

and θ_p is included as a variable in the calculation.

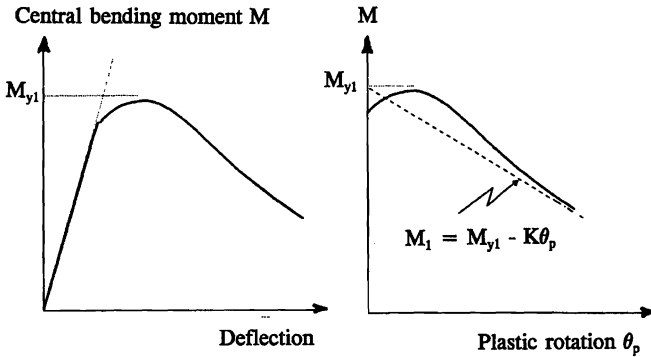


Fig.6 Interpretation of simulated central support test

It can then be shown that equations (1) and (2) remain valid with M_1 now variable and the additional equation necessary to complete the solution is

$$\frac{W_c L}{8} = M_1 + (M_{y1} - M_1) \frac{3EI}{KL} \quad (5)$$

where EI is the flexural rigidity of the purlin section.

Equations (1), (2) and (5) constitute three non-linear equations with unknowns W_c , x and M_1 which can be solved by a variety of suitable methods. The authors found both the standard procedures included in the MATHCAD software and the Newton-Raphson method entirely reliable and no doubt other techniques could also be used.

It may be noted that these equations are of more general validity than just for purlins and can advantageously be used in other similar situations, for example in the design of sheeting and decking profiles.

Numerical modelling of the behaviour at the internal support

Although the technique has not been as widely used as perhaps it should, cold-formed steel sections can be readily analyzed using shell finite elements. If elements with second-order elastic-plastic capability are used, combined buckling and yielding can be investigated. Such a procedure has been successfully used to model the behaviour of Multibeam Marks 2 and 3 at the internal support.

The elements used were 8-node isoparametric shell elements which are readily available in the literature[2]. A reduced integration scheme with 2×2 Gauss points was used for the shear and membrane strains and a 4-layer model was used to detect yield. As a consequence of the symmetry, it was only necessary to analyze half of the span. Convergence studies indicated that the mesh shown in Fig.7 was adequate with 10 to 12 elements in the length direction, depending on the span. Four of these divisions were necessary in order to model the 120 mm length adjacent to the cleat where yielding and buckling were expected to interact.

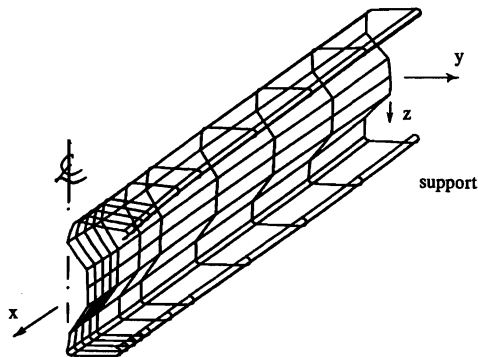


Fig.7 Finite element mesh for simulated central support calculation

Around the cross-section, the flanges, the lips and the top and bottom sections of the webs were all modelled by a single element. The middle section of the web required from 1 to 4 elements, depending on its depth so that the total number of elements necessary to model the half span varied between 130 and 224.

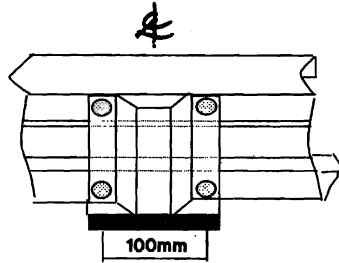


Fig.8 Cleat detail at central support

It was found that the behaviour was sensitive to the boundary conditions and care was taken to make these at both the support and the centre, where load was applied through a bolted cleat, as close to the tested conditions as possible. At the end support, the top and bottom of the web was simply supported and all nodes on the central line of symmetry were treated as sliding clamped. The cleat detail used is shown in Fig.8. The stiffness of the cleat itself was taken to be approximately infinite in the vertical direction and zero in the horizontal direction. The cleat was assumed to be rigidly connected to the member at four points, corresponding to the positions of the four bolts, at the top and bottom of the web and to provide full lateral restraint at these points. The load was assumed to be applied to the member through the cleat and the displacement was taken to be the displacement of the cleat.

For this type of analysis, it is important to take into account, at least approximately, the effect of geometrical imperfections, of strain hardening due to cold forming of the corners of the section and of residual stresses. A global imperfection in the form of a bow with the equations $y = L/1000 \sin(\pi x/2L)$ and $z = L/1000 \sin(\pi x/2L)$ was therefore incorporated in the analysis. Strain hardening was taken into account by modifying the tensile yield stress according to Karren's equation as given in the 1986 AISI Specification for the Design of Cold-Formed Structural Members[3]. Longitudinal residual stresses were included on the basis of Ingvarsson's[4] results in the form of a self-equilibrating stress pattern, tensile at the corners and compressive near the middle of the plate elements.

The material was assumed to have an idealised elastic-pure plastic stress strain relationship with Young's modulus for light gauge steel taken as 190 kN/mm^2 and Poisson's ratio as 0.3.

A typical load-deflection curve from this analysis is shown in Fig.9. It can be seen that, with appropriate deflection control, the analysis is able to accurately predict the failure moment and then to follow the drooping part of the load deflection curve well into the buckling-yielding range. The buckling configuration predicted by the computer at the end of the analysis (deflection = 57 mm) is shown in Fig.10. This is similar to the failure mode observed in the tests.

It follows that, once confidence has been established in this method of analysis, the need for simulated central support tests to establish M_{y1} and K in equation (4) is reduced or eliminated.

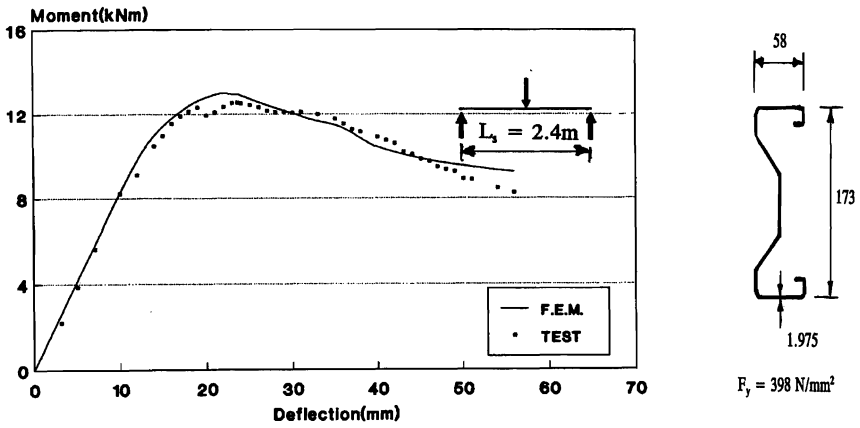


Fig.9 Experimental and theoretical load-deflection curves

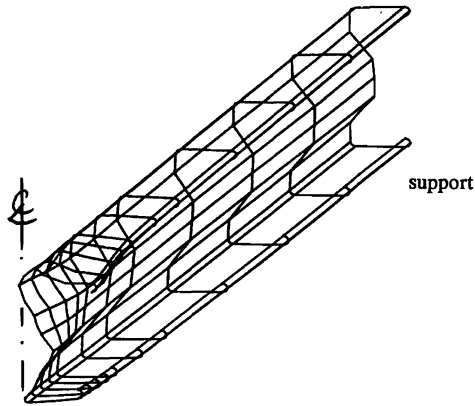


Fig.10 Buckled configuration at the conclusion of the analysis

Parametric studies using finite elements

The finite element method allows the systematic investigation of the effect of varying any of the design parameters in a way that is hardly practicable in a test series. Fig.11 shows the influence of the span $L_s = 0.4L$ on the moment-rotation relationship at an internal support. It can be seen that for relatively short spans the ultimate moment of resistance is reduced as a consequence of web buckling but that, once a certain critical span is reached, the moment-rotation relationship is independent of the span.

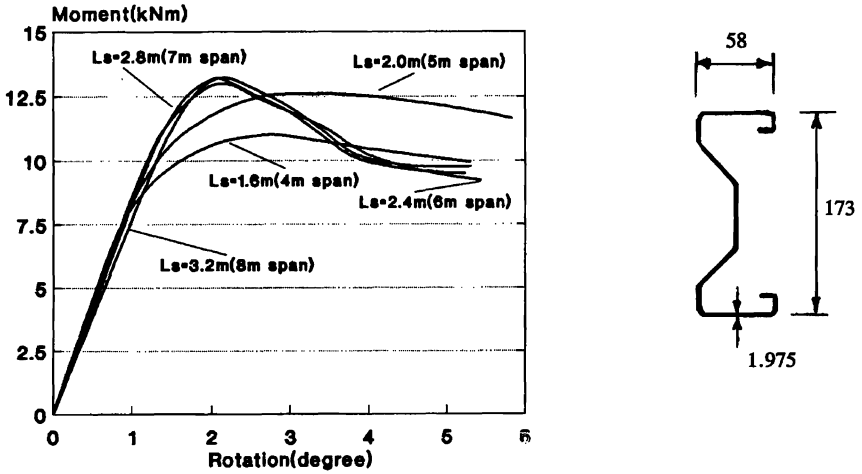


Fig.11 Results of central support tests with varying spans L_s

Fig.12 shows the influence of thickness on the moment-rotation relationship for the same section shown in Fig.11. It can be seen that the ultimate moment of resistance increases steadily with increasing thickness and that the shape of the moment-rotation curves remains very similar. In particular, the drooping parts of the curves are almost parallel which means that the constant K in equation (4) is independent of the thickness. Further parametric studies have indicated that K is approximately proportional to the height of the middle portion of the web.

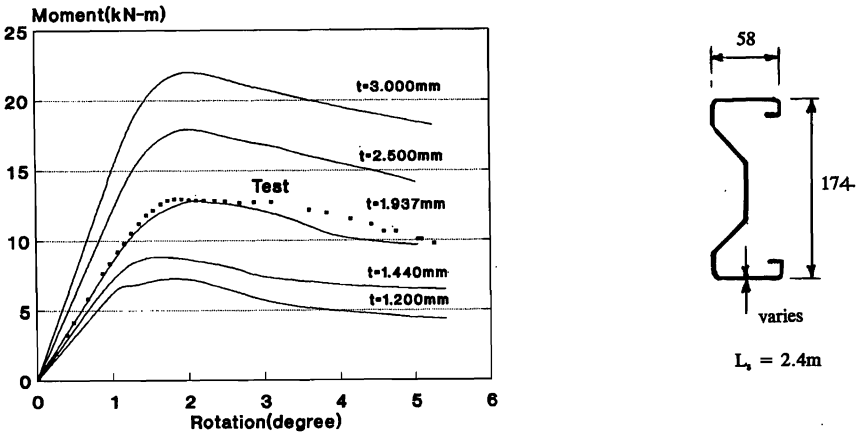


Fig.12 Central support tests with varying material thickness

Parametric studies such as these are a great help in developing empirical relationships to simplify the construction of safe load tables for families of similar sections.

Theoretical determination of the ultimate moment at mid-span

In contrast to the support moment M_1 , consideration of the ultimate moment of resistance M_2 at mid-span must take into account the restraining effect of the sheeting. M_2 has previously been obtained by testing simply-supported spans in pairs about 2 metres apart clad with a representative trapezoidal sheeting profile[1]. Separate values for both uplift and downward load are required and any consideration of different types of sheeting profiles such as standing seam or sandwich panels requires additional testing.

The moment of resistance in the span could also be calculated using non-linear shell finite elements but this would be unnecessarily expensive bearing in mind that local distortion and plasticity effects are less important here. A suitable methodology, which takes into consideration the elastic restraint from the sheeting and second-order effects, including those associated with distortion of the cross-section, is provided by Generalised Beam Theory (GBT)[5,6,7]. Space precludes a detailed description here of the application of GBT to the partially restrained buckling of cold-formed steel purlins and this is therefore given in a companion paper[8]. It is sufficient to note that GBT allows generalised section properties to be calculated which can take into account a specified elastic lateral or rotational restraint at any point in the cross-section. These section properties can then be used in an elastic buckling analysis which can include any required combination of the possible buckling modes.

The cross-sectional model for buckling analysis is therefore shown in Fig.13 and this model was used to find the elastic critical load for lateral torsional buckling making allowance where necessary for any distortion of the cross-section. For the purposes of this analysis, the beam was considered to be simply supported over a typical span and subject to a uniformly distributed vertical load. The end conditions were considered to be pinned with respect to the global lateral and torsional modes and fixed with respect to the higher-order distortional modes.

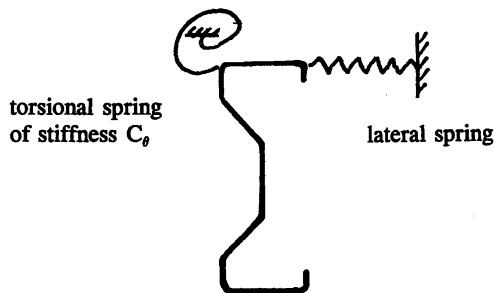


Fig.13 Cross-section model for purlin buckling analysis

It is evident that, by using appropriate values for the rotational restraint C_θ , it is possible to take account of the restraint provided by alternative cladding systems.

Having obtained the elastic critical buckling load M_{cr} in this way, the ultimate moment of resistance was calculated according to the draft Eurocode 3, Part 1.3[9], clause 6.1, thus:

$$M_2 = \chi_{LT} Z_{ef} F_y \quad (6)$$

$$\chi_{LT} = \frac{1}{\phi + \sqrt{\phi^2 - \lambda_{LT}^2}} \quad \text{but} \quad \chi_{LT} \leq 1.0 \quad (7)$$

$$\phi = 0.5[1 + 0.21(\lambda_{LT} - 0.2) + \lambda_{LT}^2] \quad (8)$$

$$\lambda_{LT} = \sqrt{\frac{Z_{ef} F_y}{M_{cr}}} \quad (9)$$

where F_y = yield stress of steel
 Z_{ef} = effective section modulus of the cross-section

Determination of the rotational restraint C_θ provided by sheeting

Sheeting provides both lateral and rotational restraint to the purlins. The lateral restraint takes the form of diaphragm (stressed skin) action which has been well documented[10]. However, sensitivity analyses indicate that it is the torsional restraint which is critical and, for cold-formed sections of open cross-section, it is sufficient to assume that the positional restraint in the plane of the sheeting is infinite.

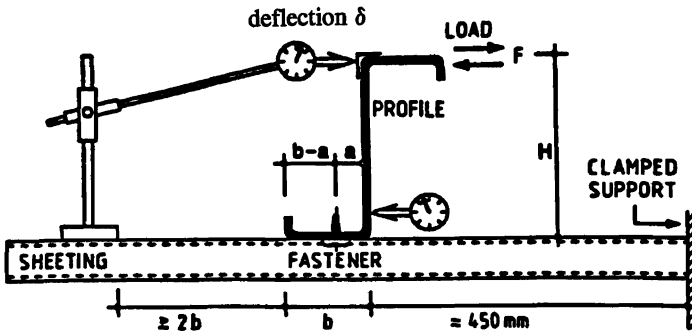


Fig.14 Procedure for 'F' test⁹

The rotational restraint C_θ can be determined either experimentally or by calculation. A suitable test procedure, often referred to as the "F-test", is described in Part 1.3 of Eurocode 3[9]. This test procedure is shown diagrammatically in Fig.14 and a total of 12 such tests were conducted on purlins of different depth in order to determine the spring stiffness C_θ for Multibeam Mark 3 with the typical roof sheeting profile used in the test series.

In Eurocode 3, the rotational stiffness is given by

$$C_\theta = \frac{D^2}{\frac{1}{K_A} + \frac{1}{K_B} - \frac{4(1 - \nu^2)D^2(c - e)}{Et^3}} \quad (10)$$

where $1/K_A + 1/K_B$ = the rotational spring stiffness F/δ determined by the F-test

- c = the developed length of the web
- a = distance of the fastener from the purlin web
- b = width of the purlin flange which is connected to the sheeting
- e = when, during the test, the contact point between the purlin and the sheeting is at the purlin web, $e = a$, while, if the contact point is at the free flange tip, $e = 2a + b$.

The 12 F-tests referred to above were carried out with the load applied in both directions so that stiffness values were obtained for both web contact and flange tip contact according to equation (10). The results obtained are shown in Fig.15 and the appropriate values were incorporated into the theoretical analysis for the ultimate span moment M_2 .

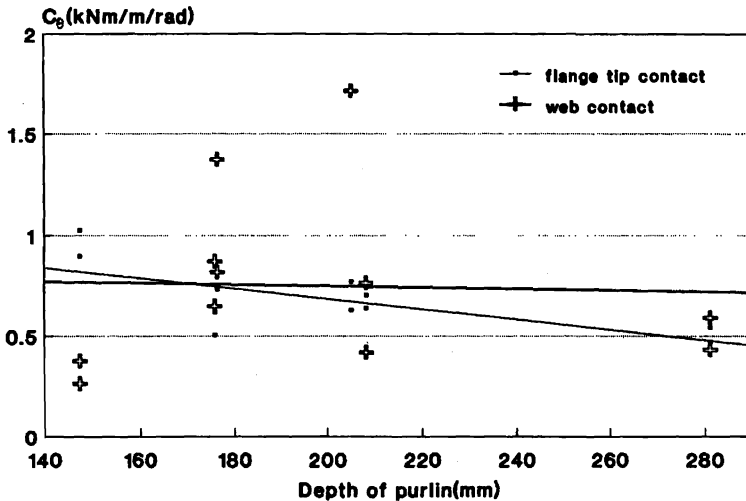


Fig.15 Results of 'F' tests on Multibeam Mark 3 purlins

Further information regarding appropriate values of the rotational stiffness C_θ for different sheeting arrangements is given in [11].

Results for a typical purlin section

The results of applying the design procedures described above to a particular cross section which has been fully tested are summarised in Table 1. The cross-section used in this study had the following dimensions and properties:

Span L	= 6.0 metres	($L_s = 2.4$ m)
Depth D	= 175 mm	
Flange width b	= 60 mm	
Thickness t	= 1.30 mm	
Yield stress F_y	= 420 N/mm ²	
Rotational stiffness C_θ	= 0.787 kNm/m/rad	

Test type	Test result	Theory	Test/theory
Simulated internal support (t = 1.975mm)	See Fig.9	See Fig.9	See Fig.9
Single span uplift	5.32 kNm	$M_{GBT} = 8.00$ kNm $M_{EC3} = 5.43$ kNm	0.980
Single span downward	7.25 kNm	$M_{GBT} = 14.91$ kNm $M_{EC3} = 7.01$ kNm	1.035
Double span uplift	10.19 kN	11.02 kN	0.924
Double span downward	13.41 kN	13.99 kN	0.959

Table 1. Test results and theory for a typical purlin section

The section for which the results are given in Table 1 was chosen because it was the only section for which a complete family of results were available at the time of writing. These were press-braked sections which lacked some of the precision expected from the rolled production. Subsequent results are proving to be significantly better, particularly for the double span uplift case. Indeed, as shown in Fig.16 later, the test/theory ratio 0.924 in table 1 is the worst result obtained to date.

Statistical correction for a family of test results

In order to provide a rational approach to the production of safe load tables valid for a range of spans, member depths and thicknesses, empirical design expressions were derived for M_{y1} , K and M_2 . As sufficient tests had been carried out, design expressions based on the test results were in fact used but they could equally have been based on numerical analysis.

These were introduced into the design equations (1), (2) and (5) and the resulting design strengths compared with the results of tests on two-span purlins subject to both uplift and downward load applied using a vacuum test rig[1]. The results of this comparison are shown in Figs.16 and 17 together with the results of a regression analysis to give a best fit straight line to the test results. It can be seen that the design procedure is essentially safe but exhibits the scatter of results that is typical of this type of design exercise.

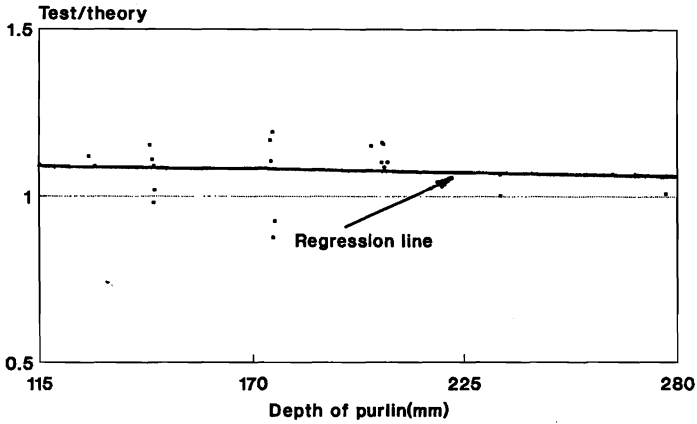


Fig.16 Comparison of theory and test for two-span purlins under uplift load

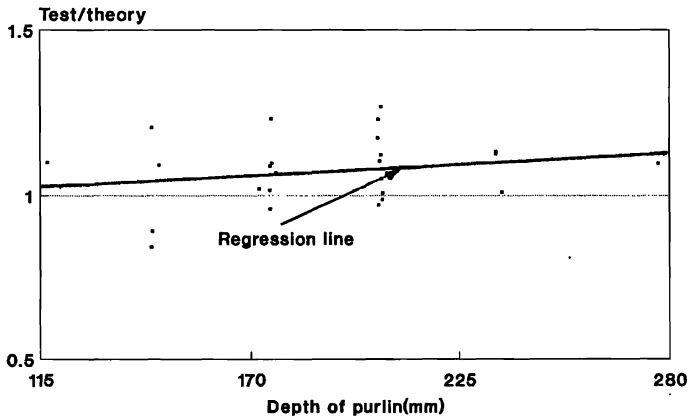


Fig.17 Comparison of theory and test for two-span purlins under downward load

In both Figs 16 and 17, the regression line provides a correction factor which is used to improve the design expression. A further statistical analysis then allows the standard deviation of the complete family of test results to be calculated and deducting approximately two standard deviations (depending on the number of tests in the family) allows a statistically reliable design expression to be determined based on the 95% fractile with a confidence limit of 75% in accordance with Eurocode 3.

Conclusions

A design procedure for a two-span purlin system has been described which is essentially based on a pseudo-plastic theory taking into account the drooping moment-rotation characteristic at the internal support. The design expressions for the ultimate bending moments at the support and at mid-span were derived on the basis of test results but it has been shown that, in each case, they could have been determined by calculation. This allows rational purlin design with the minimum of testing.

Although the method is described in terms of a simple two-span purlin system, the procedure is equally applicable to a sleeved purlin system. In each case, different sheeting arrangements can be included by an appropriate choice of the rotational restraint constant C_θ .

To date, only one representative trapezoidal sheeting profile has been included in the study but other types of cladding will be considered in due course.

A final statistical correction of the design expression against the results of two span tests was incorporated in order to give a reliable level of safety.

The results presented in the paper all refer to press-braked sections produced in advance of the cold-rolled production. The design procedure will be further refined as test results from the rolled production become available.

References

- [1] J M Davies and G Raven "Design of Cold-Formed Steel Purlins", Proc. IABSE Colloquium, Thin-Walled Metal Structures in Buildings, Stockholm, 1986, pp 151-160.
- [2] J A Figueirras and D R J Owen "Analysis of elasto-plastic and geometrically non-linear anisotropic plates and shells" in "Software for plates and shells", Eds. E Hinton and D R J Owen, Pineridge Press Ltd., 1984, pp 235-326.
- [3] "Specification for the Design of Cold-Formed Steel Structural Members", American Iron and Steel Institute, Nov. 1986.
- [4] L Ingvarsson "Cold-forming residual stress - Effect on buckling", Proc. 3rd Int Speciality Conf. on Cold-Formed Steel Structs., Univ. of Missouri-Rolla, Nov. 1975.

- [5] J M Davies and P Leach "Some applications of Generalised Beam Theory", Proc. 11th Int. Speciality Conf. on Cold-Formed Steel Structs., St. Louis, Missouri, October 1992, pp 479-501.
- [6] J M Davies and P Leach "First order generalised beam theory" Journal of Constructional Steel Research, Special Issue on cold Formed Sections, 1994.
- [7] J M Davies, P Leach and D Heinz "Second order generalised beam theory" Journal of Constructional Steel Research, Special Issue on cold Formed Sections, 1994.
- [8] J M Davies, C Jiang and P Leach "The analysis of restrained purlins using Generalised Beam Theory", 12th Int. Speciality Conf. on Cold-Formed Steel Structs., St. Louis, Missouri, October 1994.
- [9] Eurocode 3, "Design of Steel Structures", Part 1.3, "Cold formed thin gauge members and sheeting", CEN Doc. TC250/SC3/N269E, Draft approved for publication dated 25 March 1993.
- [10] J M Davies and E R Bryan "Manual of stressed skin diaphragm design", Granada, London, 1982, 441 pp.
- [11] J Lindner and T Gregull "Torsional restraint coefficients of profiled sheeting", Proc. IABSE Colloquium, Thin-Walled Metal Structures in Buildings, Stockholm, 1986, IABSE Reports, Vol. 49, pp 161-168.